

## Mid-infrared properties of a VO<sub>2</sub> film near the metal-insulator transition

H. S. Choi, J. S. Ahn, J. H. Jung, and T. W. Noh\*

*Department of Physics and Condensed Matter Research Institute, Seoul National University, Seoul 151-742, Korea*

D. H. Kim<sup>†</sup>

*Department of Electrical and Computer Engineering, State University of New York at Buffalo, Amherst, New York 14260*

(Received 16 February 1996)

A VO<sub>2</sub> film was grown on a sapphire(0001) substrate using pulsed laser deposition. The film showed a first-order metal-insulator (MI) transition and its dc conductivity started to increase drastically near 68 °C and changed by three orders of magnitude. Mid-infrared transmittance and reflectance spectra of the VO<sub>2</sub> film were measured between 20 °C and 90 °C. Using the intensity transfer-matrix method, the frequency-dependent dielectric constant  $\epsilon_f(\omega)$  and the conductivity  $\sigma_f(\omega)$  of the film were obtained between 1600 and 4000 cm<sup>-1</sup> from the measured transmittance and reflectance spectra. With the  $\epsilon_f(\omega)$  and  $\sigma_f(\omega)$  spectra, mid-infrared properties of the VO<sub>2</sub> film near the MI transition region were investigated in detail. Above 78 °C,  $\epsilon_f(\omega) < 0$  and  $d\epsilon_f/d\omega > 0$ , which is a typical metallic behavior. In particular,  $\epsilon_f(\omega)$  and  $\sigma_f(\omega)$  at 88 °C were analyzed in terms of extended Drude model in which the frequency-dependent scattering rate and the effective mass could be obtained. The mean free path of charge carriers in the dc limit was estimated to be larger by an order of magnitude than the previously reported value, i.e., 4 Å. Below 74 °C,  $\epsilon_f(\omega) > 0$  and  $d\epsilon_f/d\omega \approx 0$ , which is characteristic of an insulator. Interestingly,  $\epsilon_f$  in the insulating region increased as the temperature approached the MI transition temperature. To explain this anomalous behavior, the MI transition of the VO<sub>2</sub> film was modeled with coexistence of metallic and insulating domains and their dynamic evolution. Then the behaviors of  $\epsilon_f(\omega)$  and  $\sigma_f(\omega)$  were explained using the effective medium approximation, which is a mean-field theory predicting a percolation transition. This work clearly demonstrates that the transport and optical properties near the MI transition region are strongly influenced by the connectivity of the metallic domains. [S0163-1829(96)00231-7]

### I. INTRODUCTION

After the first observation on a metal-insulator (MI) transition in vanadium dioxide (VO<sub>2</sub>) by Morin,<sup>1</sup> this material has been intensively studied by many workers. Actually, VO<sub>2</sub> has been considered as a prototype of transition-metal oxides with intriguing MI transitions. Various physical properties related to the transition were investigated with optical,<sup>2-4</sup> structural,<sup>5,6</sup> electrical,<sup>7</sup> and magnetic measurements.<sup>7-9</sup> Also, several theoretical methods have been applied to explain the mechanism of the MI transition in VO<sub>2</sub>.<sup>10-12</sup> Despite these intense theoretical and experimental studies, some controversies on the mechanism still remain.<sup>13</sup>

The MI transition in bulk VO<sub>2</sub> occurs around 68 °C, where its dc electrical resistivity changes abruptly by more than five orders of magnitude. This transition is accompanied by a structural change from a tetragonal rutile structure in a high-temperature metallic phase to a monoclinic structure in a low-temperature insulating phase. The MI transition is a first-order phase transition, which is partly related to the structural change that involves a significant distortion of VO<sub>6</sub> octahedra and pairing of V atoms. Thermal hysteretic behaviors have been observed in numerous physical properties, but dynamic evolution, such as spinodal decomposition and domain growth, has not been studied in detail for VO<sub>2</sub>.

In this paper, temperature-dependent infrared (IR) properties of a VO<sub>2</sub> film are reported near the MI transition temperature  $T_C$ . The dielectric constant  $\epsilon_f(\omega, T)$  and the conductivity  $\sigma_f(\omega, T)$  of the VO<sub>2</sub> film were obtained from reflectance and transmittance spectra in a frequency region of 1600–4000 cm<sup>-1</sup> at temperature between 20 °C and 90 °C. It was found that  $\epsilon_f(\omega, T)$  shows an interesting behavior near  $T_C$ :  $\epsilon_f(\omega, T)$  in the insulating side increases as the temperature approaches  $T_C$ . To explain this behavior, we introduced a composite-medium model that considers the film as an inhomogeneous medium composed of metallic and insulating domains and treats the first-order phase transition as a process of domain growth. Then, the MI transition of VO<sub>2</sub> can be treated as a percolation transition. Using the effective-medium approximation, the increase of  $\epsilon_f$  near  $T_C$  could be explained and was attributed to an increase in capacitive coupling between the metallic domains. This work demonstrates that the domain growth should be taken into consideration to explain the optical properties of VO<sub>2</sub> near the MI transition regime.

The structure of this paper is as follows. In Sec. II our experimental methods, such as film deposition, dc conductivity measurements, and infrared measurements, are described. Temperature-dependent dc conductivity, and infrared reflectance and transmittance spectra of a VO<sub>2</sub> film are also shown. In Sec. III our procedure to obtain  $\epsilon_f(\omega, T)$  and  $\sigma_f(\omega, T)$  from the experimental reflectance and transmit-

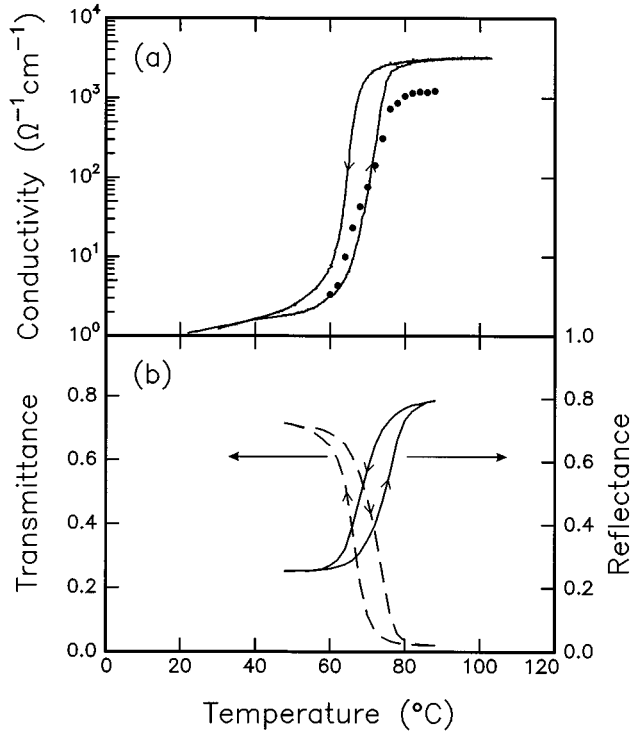


FIG. 1. (a) Temperature-dependent dc conductivity of a  $\text{VO}_2$  film and (b) temperature dependence of reflectance (solid lines) and transmittance (dashed lines) of the film at  $2000\text{ cm}^{-1}$ . Solid circles in (a) show its infrared conductivity at  $2000\text{ cm}^{-1}$  during heating process. The thermal hysteresis behaviors indicate that the film undergoes a first-order phase transition.

tance spectra is described in detail. Optical constants of a sapphire substrate as well as the  $\text{VO}_2$  film are presented. In Sec. IV,  $\epsilon_f(\omega, T)$  and  $\sigma_f(\omega, T)$  in the IR region are discussed. Our findings are summarized in Sec. V.

## II. EXPERIMENT

### A. Deposition of $\text{VO}_2$ films

$\text{VO}_2$  films were grown on sapphire(0001) substrates with pulsed laser deposition using an ArF excimer laser. Intense light pulses at a wavelength of 193 nm were focused onto a  $\text{VO}_2$  target with a fluence of  $2\text{--}3\text{ J/cm}^2$ . A base pressure inside a deposition chamber was less than  $10^{-5}$  Torr and an ambient condition during the deposition was  $20\text{--}30\text{ mTorr}$  of oxygen. The films were deposited at  $630\text{ }^\circ\text{C}$  and then cooled down to room temperature at the deposition oxygen pressure without further post annealing. The thickness of the film used in this IR study was about  $1500\text{ \AA}$ . An x-ray-diffraction study revealed that most of the film is composed of the  $\text{VO}_2$  phase, but with a very small amount of a secondary phase. In addition, the film is highly oriented with its monoclinic (010) plane parallel to the substrate surface. Details of growth and characterization of the films were published elsewhere.<sup>14</sup>

### B. dc conductivity measurements

The dc conductivity of the  $\text{VO}_2$  film was measured using a conventional four-probe method. Figure 1(a) shows

temperature-dependent dc conductivity  $\sigma_{\text{dc}}(T)$ . As the temperature increases,  $\sigma_{\text{dc}}(T)$  starts to increase abruptly around  $68\text{ }^\circ\text{C}$  and changes by more than three orders of magnitude. Compared to the MI transition region of single crystal  $\text{VO}_2$ ,<sup>7</sup> that of the film is a little bit broader, possibly due to defects inside the film. Figure 1(a) also shows a thermal hysteresis effect, and temperature difference between the heating and cooling curves is found to be about  $8\text{ }^\circ\text{C}$ . This hysteretic behavior demonstrates that our film undergoes a first-order phase transition.

### C. IR measurements

Both reflectance and transmittance spectra of the  $\text{VO}_2$  film were measured in a spectral range between  $450$  and  $4000\text{ cm}^{-1}$  using a Fourier transform spectrophotometer. The experimental resolution was  $8\text{ cm}^{-1}$ . Since the MI transition of the film shows a thermal hysteresis, it would be ideal to measure reflectance and transmittance spectra simultaneously. However, we could not perform such simultaneous measurements due to our experimental configuration. Instead, we tried to minimize experimental errors by monitoring the sample temperature carefully. The  $\text{VO}_2$  film was mounted on a heating block, whose temperature could be controlled by two cartridge heaters, a  $K$ -type thermocouple, and a controlling unit. To suppress unnecessary blackbody radiation from the heating block entering to a detector, a water-cooled copper jacket was built around the block. To measure the sample temperature accurately, a separate  $K$ -type thermocouple was attached to one corner of the film. During one thermal cycle between  $20\text{ }^\circ\text{C}$  and  $90\text{ }^\circ\text{C}$ , reflectance  $\mathcal{R}(\omega, T)$  was measured with an incident angle of  $8^\circ$ . Then the heating block was positioned for transmission measurements, where the light entered normal to the film. Transmittance  $\mathcal{T}(\omega, T)$  was measured during another thermal cycle between  $20\text{ }^\circ\text{C}$  and  $90\text{ }^\circ\text{C}$ . The reflectance and transmittance spectra were measured at every  $2\text{ }^\circ\text{C}$  and the sample temperature was stabilized within  $\pm 0.2\text{ }^\circ\text{C}$  before taking the spectra. The rate of temperature change was maintained the same for both thermal cycles.

$\mathcal{R}(2000\text{ cm}^{-1}, T)$  and  $\mathcal{T}(2000\text{ cm}^{-1}, T)$  during the thermal cycles are shown in Fig. 1(b).<sup>15</sup> Both of these quantities show hysteretic behaviors, which are similar to that of the dc resistivity. Note that the film is transparent in the mid-IR region below  $60\text{ }^\circ\text{C}$  and becomes opaque above  $80\text{ }^\circ\text{C}$ . This sudden change of the transmittance was already observed by earlier workers<sup>16,17</sup> and is the reason why  $\text{VO}_2$  films have been studied extensively for applications of optical switches and infrared sensors.

Figure 2 shows the reflectance and transmittance spectra of the  $\text{VO}_2$  film at some selected temperatures during a heating process. Around  $60\text{ }^\circ\text{C}$ , the film is insulating and the light is able to penetrate the  $\text{VO}_2$  thin layer, so the overall features of  $\mathcal{R}$  and  $\mathcal{T}$  spectra are mainly determined by the sapphire substrate. As temperature increases,  $\mathcal{R}$  increases and  $\mathcal{T}$  decreases. Moreover, phonon structures in the reflectance spectra become weak due to screening of free carriers generated in the metallic phase.

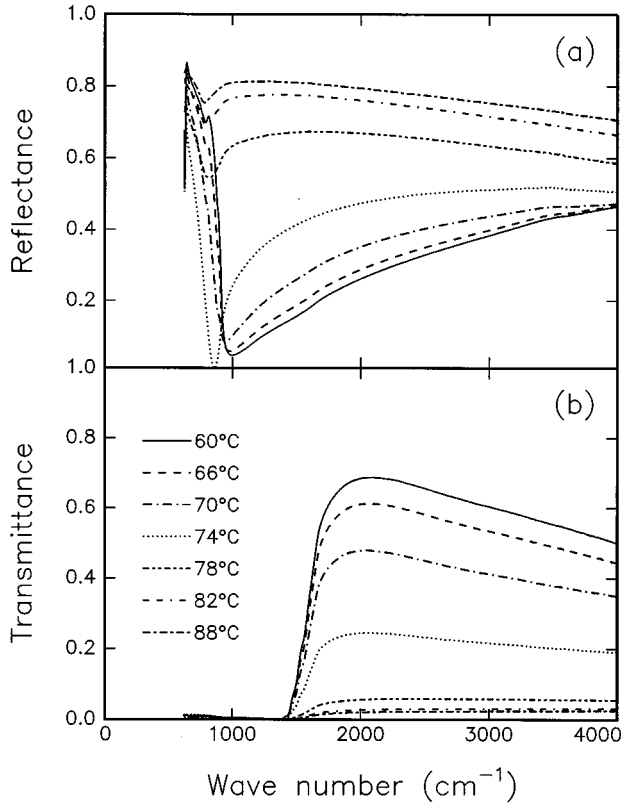


FIG. 2. (a) Reflectance and (b) transmittance spectra of the VO<sub>2</sub> film at selected temperatures during the heating process.

### III. DETERMINATION OF OPTICAL CONSTANTS OF THE VO<sub>2</sub> FILM

#### A. Other spectroscopic methods

To determine optical constants of a bulk sample, a Kramers-Kronig analysis on measured reflectance is frequently used. In this method, a reflectance spectrum is measured in a wide frequency region and a phase shift due to reflection is determined using the Kramers-Kronig relation.<sup>18</sup> For such a calculation, reflectance data from zero to infinity frequency should be known, so proper extrapolation schemes should be used for the frequency regions where reflectance data are not available.<sup>19</sup> Moreover, in a film geometry, the phase shift of the reflected light is a complicated function of numerous physical quantities, such as optical constants and a thickness of a film and those of a substrate, so the Kramers-Kronig analysis might be difficult to apply.

In ellipsometry, polarization-dependent reflectance spectra are measured for a light entering obliquely near the Brewster angle.<sup>20</sup> Since more than two quantities can be measured at a single frequency, there is no need for extrapolations and optical constants can be determined more accurately. This method can also be applied to a film geometry. However, ellipsometric measurements in the mid-IR region have not been well established yet, due to lack of proper polarizing elements. Therefore, we had to rely on other technique that use both the reflectance and transmittance spectra to get the optical constants of the VO<sub>2</sub> film.

#### B. The intensity transfer-matrix method

To determine refractive index  $n_f(\omega, T)$  and extinction coefficient  $k_f(\omega, T)$  of the VO<sub>2</sub> film from  $\mathcal{R}(\omega, T)$  and

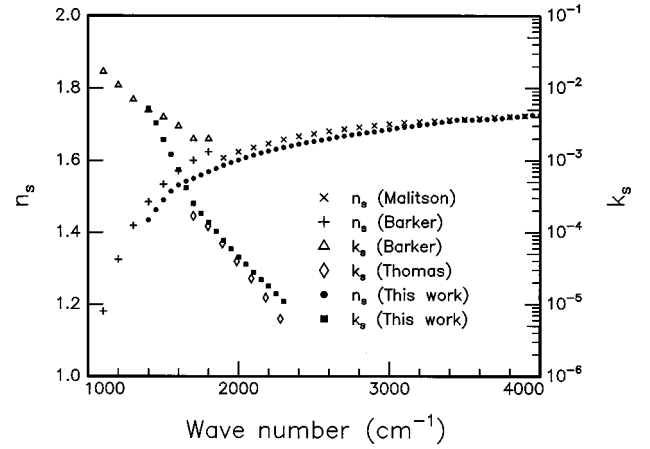


FIG. 3. Room-temperature values of  $n_s(\omega)$  and  $k_s(\omega)$  for the sapphire substrate. Our data, which were derived using the ITMM, are compared with other reported values of Malitson, Murphy, and Rodeny (Ref. 24), Barker (Ref. 25), and Thomas, Joseph, and Tropf (Ref. 26).

$\mathcal{T}(\omega, T)$ , proper relations between these physical quantities should be established. For our experimental configurations,  $\mathcal{R}$  and  $\mathcal{T}$  can be written in terms of  $n_f$  and  $k_f$  using a set of proper Fresnel equations.<sup>21</sup> In a film geometry, Fabry-Pérot fringes frequently appear in  $\mathcal{R}$  and  $\mathcal{T}$  spectra due to interference of multiply reflected beams from parallel substrate surfaces. However, the spectra in Fig. 2 do not show such interference fringes, partly due to the low experimental resolution and to a small misalignment between the parallel substrate surfaces. To explain the lack of the Fabry-Pérot fringes in the  $\mathcal{R}$  and  $\mathcal{T}$  spectra, the phase information between the multiply reflected beams should be neglected and the beams should be added incoherently. A systematic treatment for such an incoherent addition is called the ‘‘intensity transfer-matrix method’’ (ITMM) and has been applied to calculate the optical constants of numerous films.<sup>21–23</sup>

Under this approximation,  $\mathcal{R}$  and  $\mathcal{T}$  can be given as functions of  $n_f$  and  $k_f$  and the film thickness  $t$  when the optical constants and thickness of the substrate are known, i.e.,  $\mathcal{R} = \mathcal{R}(n_f, k_f; t)$  and  $\mathcal{T} = \mathcal{T}(n_f, k_f; t)$ . The detailed expressions<sup>21</sup> under the ITMM are highly complicated and nonlinear, so  $n_f$  and  $k_f$  cannot be written as analytic functions of  $\mathcal{R}$  and  $\mathcal{T}$ . Therefore, we had to rely on a numerical method to find  $n_f$  and  $k_f$  from the measured  $\mathcal{R}$  and  $\mathcal{T}$  spectra.

#### C. Optical constants of the sapphire substrate

To apply the ITMM, the refractive index  $n_s$  and the extinction coefficient  $k_s$  of the substrate should be known. Since the substrate is a **c**-cut sapphire,  $n_s$  and  $k_s$  in **ab** plane should be used. Sapphire has a hexagonal structure and its optical constants have an uniaxial anisotropy, so the optical constants along the **a** and **b** axes should be the same. Since the incident angle was small, i.e., about 8°, in our reflectance measurements, a small contribution from an extraordinary ray (i.e.,  $\vec{E}$  is parallel to the **c** axis) was not taken into account in our analysis.

As shown in Fig. 3, reported values of  $k_s$  for the sapphire **ab** plane around 2000 cm<sup>-1</sup> vary quite a lot.<sup>24–27</sup> To get

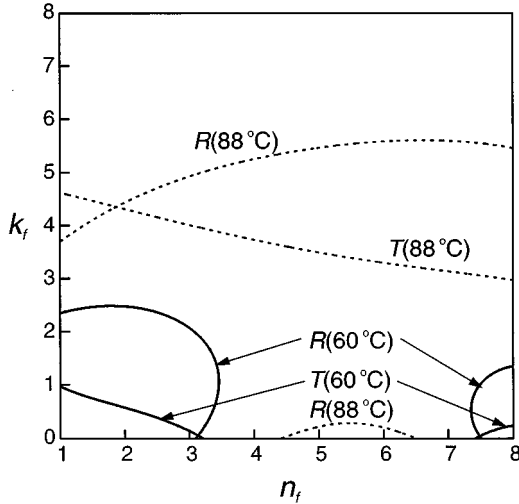


FIG. 4. Contour map formed by curves that correspond to the measured values of the reflectance and the transmittance at  $4000 \text{ cm}^{-1}$ . The complex refractive index ( $n_f, k_f$ ) at a given temperature is determined from the intersecting points of the reflectance and transmittance curves at the given temperature.

$n_s$  and  $k_s$ , we measured reflectance and transmittance spectra of a sapphire substrate at room temperature and performed numerical calculations using the ITMM. Our measured values of  $n_s$  and  $k_s$  were found to be similar to those reported in Refs. 24 and 26, respectively. The significant  $k_s$  value in the mid-infrared region was attributed to the multiphonon absorption process.<sup>26,27</sup> (For the ordinary ray direction, the bulk sapphire has TO phonons at 385, 442, 569, and  $653 \text{ cm}^{-1}$  and LO phonons at 388, 480, 625, and  $900 \text{ cm}^{-1}$ .<sup>28</sup>) According to literature on optical properties of sapphire,<sup>26,27</sup> the changes of  $n_s$  and  $k_s$  between 295 and 363 K were known to be very small. In fact, we measured temperature-dependent spectra of reflectance and transmittance for the sapphire substrate and found that their changes were smaller than 0.5% between room temperature and  $100^\circ \text{C}$ . Therefore, the temperature dependences of  $n_s$  and  $k_s$  could be neglected in our data analysis.

#### D. Optical constants of the $\text{VO}_2$ film

It should be noted that it is possible to have more than one solution of  $n_f(\omega, T)$  and  $k_f(\omega, T)$  corresponding to measured values of  $\mathcal{R}(\omega, T)$  and  $\mathcal{T}(\omega, T)$ . Therefore, a proper solution should be chosen using reasonable physical grounds and continuity of  $n_f$  and  $k_f$  with respect to  $\omega$ . Figure 4 shows contour curves in ( $n_f, k_f$ ) space for given values of  $\mathcal{R}$  and  $\mathcal{T}$  at  $4000 \text{ cm}^{-1}$ . Solid lines show contours for the measured values of  $\mathcal{R}$  and  $\mathcal{T}$  at  $60^\circ \text{C}$ , i.e., on the insulating side. These lines run across at two points in ( $n_f, k_f$ ) space, i.e.,  $n_f \approx 3.1$  or  $7.5$  and  $k_f \approx 0.0$ . From reported IR data<sup>3</sup> on a single-crystal  $\text{VO}_2$ ,  $n_f(4000 \text{ cm}^{-1}, 293 \text{ K})$  is estimated to be located between 3.0 and 4.0, so the solution of  $n_f \approx 3.1$  is a proper one. The dashed lines in Fig. 4 show contour lines for the measured values of  $\mathcal{R}$  and  $\mathcal{T}$  at  $88^\circ \text{C}$ , i.e., on the metallic side. Though there are two contour lines for the measured  $\mathcal{R}$  value, there is only one solution at  $n_f \approx 1.9$  and  $k \approx 4.3$ .

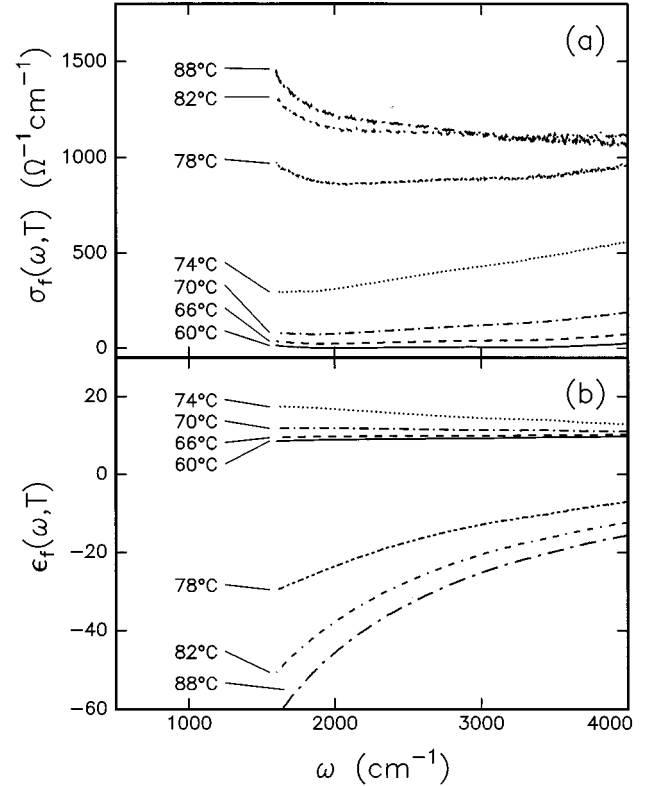


FIG. 5. (a) Infrared conductivity and (b) infrared dielectric constant, obtained from the experimental reflectance and transmittance spectra using the ITMM.

Since  $n_f < k_f$ , the dielectric constant of the film  $\epsilon_f \equiv n_f^2 - k_f^2$  becomes negative, consistent with the fact that  $\text{VO}_2$  becomes metallic at  $88^\circ \text{C}$ .

When  $\mathcal{R}$  or  $\mathcal{T}$  becomes very small, experimental errors of  $n_f$  and  $k_f$  become very large. Therefore, the spectral range of this study was limited by phonon absorption in the sapphire substrate. The multiphonon process in the sapphire substrate makes  $k_s$  large enough to result in a very small transmittance below  $1450 \text{ cm}^{-1}$ , as shown in Fig. 2(b). In addition, the large change in  $\mathcal{T}$  between 1450 and  $1600 \text{ cm}^{-1}$  can also provide large errors in determining  $n_f$  and  $k_f$ . So, in this study,  $n_f$  and  $k_f$  were determined in the frequency region above  $1600 \text{ cm}^{-1}$ .

Figure 5 shows the results of the ITMM analysis for the  $\text{VO}_2$  film. The IR conductivity  $\sigma_f(\omega, T)$  and the IR dielectric constant,  $\epsilon_f(\omega, T)$  are shown at some selected temperatures in the MI transition region. Note that  $\sigma_f$  and  $\epsilon_f$  shown in this figure were obtained from the  $\mathcal{R}$  and  $\mathcal{T}$  spectra during the heating process.<sup>29</sup> At  $T = 60^\circ \text{C}$ , which is below  $T_C$ , the film displays a typical insulatorlike behavior:  $\sigma_f$  is very small and  $\epsilon_f$  is positive and nearly constant (i.e., about 10) in the IR region. On the contrary, at  $T = 88^\circ \text{C}$ , which is above  $T_C$ , the film shows a typical metallic behavior:  $\sigma_f$  becomes large and  $\epsilon_f$  is negative. As  $\omega$  becomes smaller,  $|\epsilon_f(\omega, T)|$  becomes larger.

## IV. RESULTS AND DISCUSSIONS

### A. Infrared conductivity in metallic $\text{VO}_2$

Figure 5(a) shows that the IR conductivity increases as  $T$  is raised. To check the correlation between the infrared and

dc conductivities, values of  $\sigma_f(2000 \text{ cm}^{-1}, T)$  during the heating process are plotted as solid circles in Fig. 1(a). It can be easily noticed that the behavior of  $\sigma_f(2000 \text{ cm}^{-1}, T)$  is highly correlated with that of  $\sigma_{dc}(T)$ , suggesting that the change in the IR conductivity is closely related to the generation of free carriers at the MI transition.

A model that includes this free-carrier contribution is the simple Drude model, where the complex dielectric constant  $\tilde{\epsilon}_f \equiv \epsilon_f + (i4\pi/\omega)\sigma_f$  of the VO<sub>2</sub> film in the metallic regime can be written as

$$\tilde{\epsilon}_f(\omega) = \epsilon_\infty \left\{ 1 - \frac{\tilde{\omega}_p^2}{\omega(\omega + i\Gamma)} \right\} = \epsilon_\infty - \frac{4\pi Ne^2}{m^*} \frac{1}{\omega(\omega + i\Gamma)}. \quad (1)$$

$\epsilon_\infty$  represents the high-frequency dielectric constant coming from interband transitions and  $\tilde{\omega}_p$ ,  $\Gamma$ ,  $N$ , and  $m^*$  are the screened plasma frequency, scattering rate, density, and effective mass of free carriers, respectively. Barker *et al.*<sup>2</sup> suggested that  $\tilde{\omega}_p = 9 \times 10^3 \text{ cm}^{-1}$ ,  $\Gamma = 10 \times 10^3 \text{ cm}^{-1}$ , and  $\epsilon_\infty = 9$  from a Kramers-Kronig analysis on reflectance data of a VO<sub>2</sub> single crystal.

Figures 6(a) and 6(b) show the IR dielectric constant and conductivity of the VO<sub>2</sub> film at  $T = 88^\circ\text{C}$ , respectively. Experimental data are denoted with solid circles. Dashed lines are the predictions of the simple Drude model when parameters suggested by Barker *et al.* are used. It is evident that there are large discrepancies between the experimental data and the theoretical predictions. The simple Drude model can provide a good fit to the experimental  $\epsilon_f(\omega, 88^\circ\text{C})$  data, shown as dotted line in Fig. 6(a):  $\tilde{\omega}_p = 7.8 \times 10^3 \text{ cm}^{-1}$ ,  $\Gamma = 2.5 \times 10^3 \text{ cm}^{-1}$ , and  $\epsilon_\infty = 9$ . However, in this case, the experimental value of  $\sigma_f(\omega, 88^\circ\text{C})$  cannot be explained reasonably well with the same parameters.

To make a better explanation<sup>30</sup> the spectra were analyzed in terms of extended Drude model, which has the same expression as Eq. (1) but with frequency-dependent scattering rate  $\Gamma(\omega)$  and effective mass  $m^*(\omega)$ . For a given frequency, the values of  $\Gamma(\omega)$  and  $m^*(\omega)$  can be uniquely determined from the experimental optical constants, when the value of  $N$  is known. With a reported value<sup>2</sup> of the carrier density, i.e.,  $N = 3.0 \times 10^{21} \text{ cm}^{-3}$ ,  $\Gamma(\omega)$  and  $m^*(\omega)$  were determined from the measured values of  $\epsilon_f(\omega, 88^\circ\text{C})$  and  $\sigma_f(\omega, 88^\circ\text{C})$ . Figure 6(c) shows that  $\Gamma(\omega)$  increases but that  $m^*(\omega)$  decreases, as frequency increases, which is a typical behavior of a highly correlated electron system.<sup>31,32</sup>

$\Gamma(\omega = 2000 \text{ cm}^{-1})$  of the VO<sub>2</sub> film is about  $1500 \text{ cm}^{-1}$ , larger than that of a good metal (typically, about  $500 \text{ cm}^{-1}$ ). Since the scattering rate is comparable to the frequency, the IR conductivity at  $2000 \text{ cm}^{-1}$  is closely related to the dc conductivity, as shown in Fig. 1(a).

It should be noted that  $\Gamma(\omega)$  in Fig. 6(c) is much smaller than the value of the scattering rate obtained by Barker *et al.*, i.e.,  $\Gamma = 10 \times 10^3 \text{ cm}^{-1}$ . The scattering rate is closely related to the mean free path  $l$  of carriers.<sup>33</sup> The parameters of Barker *et al.* provide that  $l \sim 4 \text{ \AA}$ , which is clearly too short for the metallic state. Recently, Allen *et al.*<sup>34</sup> studied high-temperature resistivity of VO<sub>2</sub>. They showed that the short mean free path value based on  $\Gamma = 10 \times 10^3 \text{ cm}^{-1}$  gives an

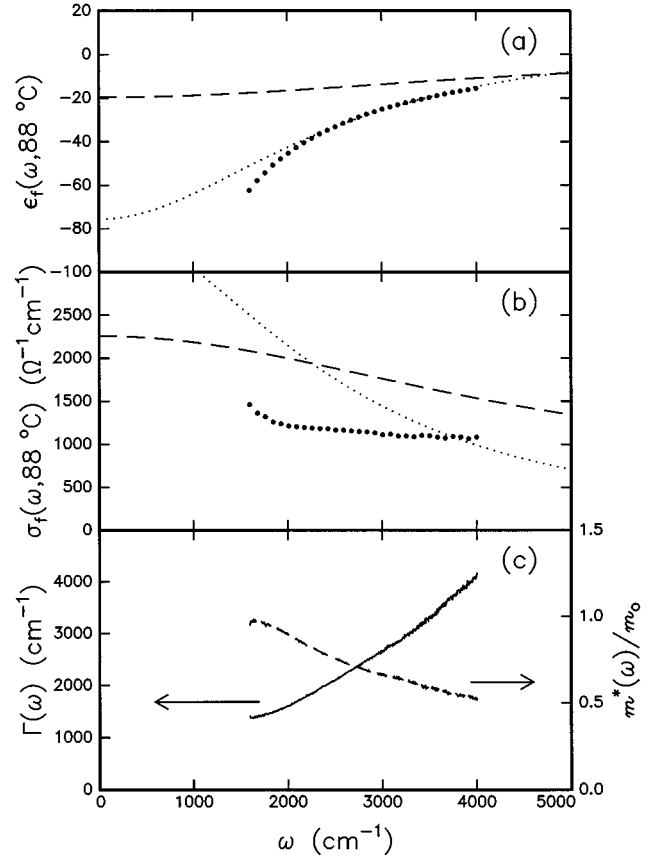


FIG. 6. (a) Dielectric constant and (b) conductivity of the VO<sub>2</sub> film at  $88^\circ\text{C}$  (i.e., in the metallic region). The solid circles represent our experimental data. The dashed lines are the predictions of the simple Drude model with parameters suggested by Barker *et al.* The dotted lines are the predictions of the simple Drude model when the parameters are adjusted to fit the measured  $\epsilon_f(\omega)$ . In (c), the frequency-dependent scattering rate  $\Gamma$  (solid line) and the effective-mass ratio  $m^*/m_0$  (dashed line), which are derived in the extended Drude model, are shown.

internal inconsistency in the conventional Bloch-Boltzmann interpretation. They attributed this inconsistency either to unknown internal damages inside a VO<sub>2</sub> sample or to nonapplicability of the conventional Fermi liquid model. In Fig. 6(c), values of  $\Gamma$  and  $m^*$  are given only in the mid-IR region, so then dc values cannot be determined exactly. However, when their dc values are estimated as  $\Gamma \sim 1000 \text{ cm}^{-1}$  and  $m^*/m_0 \sim 1.5$ ,  $l$  will be about  $100 \text{ \AA}$ . Note that these values are only approximate estimations. However, it is clear that  $l$  is larger by about an order of magnitude than  $4 \text{ \AA}$ . This large value of  $l$  removes the inconsistency observed by Allen *et al.*<sup>34</sup>

## B. Behavior of $\epsilon_f$ of the insulating VO<sub>2</sub> film

The temperature dependence of  $\epsilon_f$ , shown in Fig. 5(b), is quite interesting. Above  $80^\circ\text{C}$ ,  $\epsilon_f(\omega)$  is approximately proportional to  $-1/\omega^2$ , which is a typical behavior for Drude carriers. As  $T$  increases in the metallic side,  $\epsilon_f$  decreases. However, as  $T$  approaches  $T_C$  in the insulating side,  $\epsilon_f$  increases. This increment of  $\epsilon_f$  cannot be explained by a simple increase of  $N$  in the simple or extended Drude model.

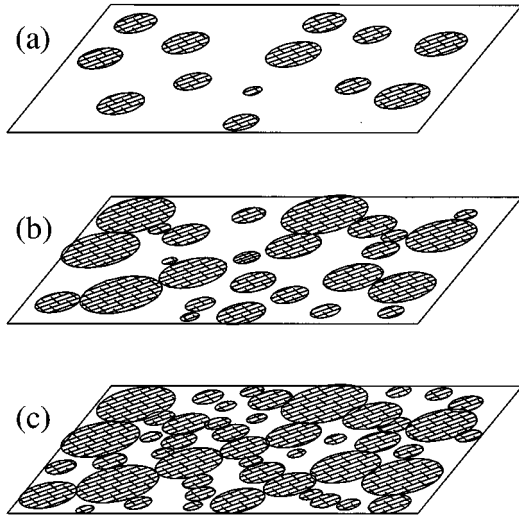


FIG. 7. Schematic diagram of the MI transition in the  $\text{VO}_2$  film. (a) The metallic domains start to form nucleation droplets in the film surface sporadically, as  $T$  approaches  $T_C$ . (b) The domains grow larger and start to form clusters as  $T$  increases further. (c) Above  $T_C$ , the metallic domains form an infinite cluster.

An increase of the dielectric constant on the insulating side near the MI transition region has appeared in numerous models.<sup>35,36</sup> According to the Herzfeld criterion,<sup>35,36</sup> valence electrons are considered to be localized around nuclei and contribute to atomic polarizability. Near the MI transition, the polarizability diverges, so the dielectric constant should diverge. Above the transition, the restoring force of the valence electrons vanishes, resulting in free carriers. Another model that predicts the increase of  $\epsilon_f$  near the MI transition is the Anderson localization model.<sup>36</sup> A polarizability of a medium is proportional to square of localization length, i.e., a typical size of the localized wave function. Since the localization length diverges near the MI transition,  $\epsilon_f$  should diverge. (However, it is clear that the MI transition in  $\text{VO}_2$  is not induced by disorder.)

Note that both of the above microscopic models deal with dielectric constants mainly in dc limit, so our mid-IR data could not be explained. In addition, it is difficult to include the first-order nature of the MI transition in  $\text{VO}_2$ . Instead of relying on microscopic models, we will deal with a composite model that takes into account the evolution of domain growth during the first-order transition. Then, the increase of  $\epsilon_f$  near the MI transition can be interpreted as a dielectric anomaly related to percolation.

### C. A composite medium model

In the first-order transition of  $\text{VO}_2$ , the low-temperature insulating phase can exist above  $T_C$  as a metastable phase and the high-temperature metallic phase can also exist below  $T_C$ . These will bring thermal hysteretic behaviors in numerous physical properties of  $\text{VO}_2$ , as shown in Fig. 1. As  $T$  is raised, domains of the metallic phase begin to form nucleation droplets in the film sporadically, as shown in Fig. 7(a). In contrast to a second-order phase transition where there is a sudden transition from one phase to another, there is an in-

stability (called the ‘‘spinodal decomposition’’) against the infinitesimal amplitude and nonlocalized fluctuations that result in a phase separation. When  $T$  increases further, the domains of the metallic phase start to form clusters, as shown in Fig. 7(b). When  $T$  is far above  $T_C$ , the conducting clusters become larger and form a conducting path throughout the film, as shown in Fig. 7(c). This is quite similar to percolation transitions observed in various metal-insulator composites.<sup>37</sup>

To include the effect of the domain growth, the  $\text{VO}_2$  film should be described as an *inhomogeneous* composite medium composed of metallic and insulating grains. Then, optical properties of the inhomogeneous medium can be modeled by effective-medium theories, which predict the effective dielectric constant of the composite medium in terms of dielectric constants and volume fractions of its constituent components. The effective-medium approximation (EMA), developed by Bruggeman<sup>38</sup> and generalized by Stroud,<sup>39</sup> has been widely used to explain optical properties of composites that have percolation transitions.<sup>40</sup>

In the EMA, it is assumed that individual grains, either metallic or insulating, are considered to be embedded in a uniform background, i.e., an ‘‘effective medium,’’ which has average properties of the mixture. A self-consistent condition<sup>41</sup> such that the total depolarization field inside the inhomogeneous medium is equal to zero leads to a quadratic equation for effective dielectric constant  $\tilde{\epsilon}_{\text{eff}}$ ,

$$f_m \frac{\tilde{\epsilon}_m - \tilde{\epsilon}_{\text{eff}}}{\tilde{\epsilon}_m + (d-1)\tilde{\epsilon}_{\text{eff}}} + f_i \frac{\tilde{\epsilon}_i - \tilde{\epsilon}_{\text{eff}}}{\tilde{\epsilon}_i + (d-1)\tilde{\epsilon}_{\text{eff}}} = 0, \quad (2)$$

where  $\tilde{\epsilon}_m$  and  $\tilde{\epsilon}_i$  represent the complex dielectric constants of the metallic and insulating  $\text{VO}_2$  phases, respectively. In addition,  $f_m$  and  $f_i$  ( $= 1 - f_m$ ) represent volume fractions of the metallic and insulating grains, respectively. Since the thickness of the film was estimated to about 1500 Å, the dimensionality of the composite medium  $d$  was set to 2. Note that the EMA equation predicts a percolation at  $f_m = 0.5$  in two dimension, where an infinite cluster of the metallic  $\text{VO}_2$  is formed.

To apply the EMA, it was assumed that  $\tilde{\epsilon}_m(\omega)$  and  $\tilde{\epsilon}_i(\omega)$  could be represented by the values of the  $\text{VO}_2$  film at 88 and 60 °C, respectively; in other words,  $\tilde{\epsilon}_m(\omega) = \tilde{\epsilon}_f(\omega, 88^\circ\text{C})$  and  $\tilde{\epsilon}_i(\omega) = \tilde{\epsilon}_f(\omega, 60^\circ\text{C})$ . Figure 8 shows the EMA predictions for the effective conductivity and the effective dielectric constant for various values of  $f_m$ . This figure shows good agreement with the experimental results, shown in Fig. 5. Note that the figure predicts not only the MI transition of the  $\text{VO}_2$  film but also the anomalous increase of  $\epsilon_f$  below  $f_m = 0.5$ .

Figure 9 shows a plot of  $\epsilon_f(2000\text{ cm}^{-1}, T)$  vs  $\sigma_f(2000\text{ cm}^{-1}, T)$  for the  $\text{VO}_2$  film. The experimental data at every 2 °C are shown as solid circles. Below 76 °C, the dielectric constant becomes larger near the MI transition. The EMA predictions are also shown as the solid line, along which the volume fraction of the metallic phase is marked. From this figure, we can estimate  $f_m$  at each temperature. In the insulating region between 60 °C and 74 °C,  $f_m$  is estimated to vary from 0.00 to 0.25. In addition, in the metallic region between 78 °C and 88 °C,  $f_m$  is estimated to change

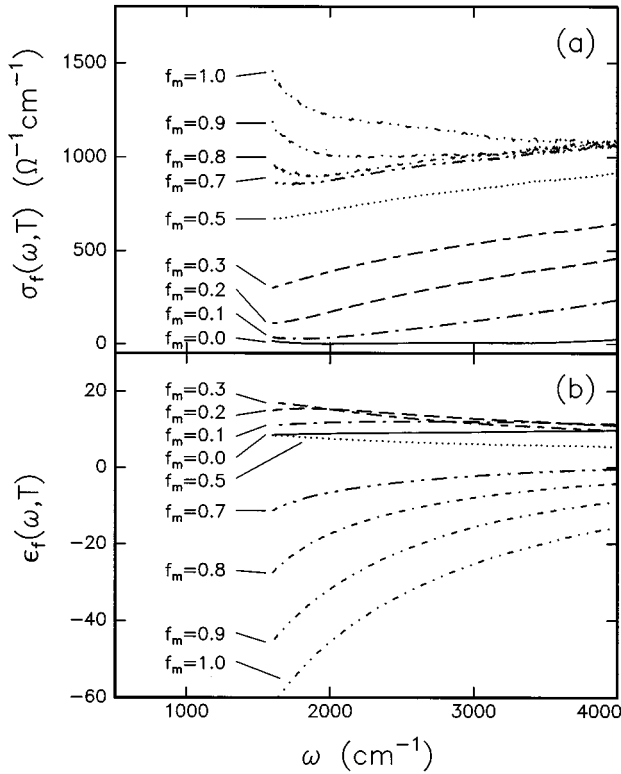


FIG. 8. (a) IR conductivity and (b) IR dielectric constant predicted by the two-dimensional EMA, which is a mean-field theory predicting the percolation transition.

from 0.85 to 1.00. There is a significant change in  $f_m$  between 74 °C and 78 °C and the percolation threshold should be located at this temperature region. The existence of the percolation threshold can be also induced from the frequency dependencies of  $\sigma_f$  and  $\epsilon_f$ , shown in Fig. 5.<sup>42</sup> The conductivity of the film below 2000 cm<sup>-1</sup> shows that  $d\sigma_f/d\omega > 0$  below 74 °C and  $d\sigma_f/d\omega < 0$  above 78 °C. The dielectric constant of the film shows that  $d\epsilon_f/d\omega \approx 0$  below 74 °C and  $d\epsilon_f/d\omega > 0$  above 78 °C.

The increase of  $\epsilon_f$  near the MI transition can be understood in the percolation model. Near the percolation, effective capacitive coupling between the metallic clusters increases due to an increase in the effective area and a decrease in the spacing between the metallic clusters. This increment of the coupling will result in the increase of dielectric constant near the percolation transition. This effect has been observed by Grannan *et al.*<sup>43</sup> in a Ag-KCl composite at a low frequency of 1 KHz. It is quite interesting that such an effect still exists in the infrared region, as illustrated in this work.

From Fig. 9 it is clear that the EMA can explain the optical constants of the VO<sub>2</sub> film quite well in most temperature regions. The deviation near the MI transition, i.e., 76 °C, can be understood from the fact that the EMA is a mean-field approximation, whose description in a critical region is quite poor.<sup>44</sup> The reasonably good agreement between the experimental data and the EMA predictions demonstrates that physical properties of a material near a first-order phase transition temperature should be understood in terms of a composite medium theory. A simple treatment

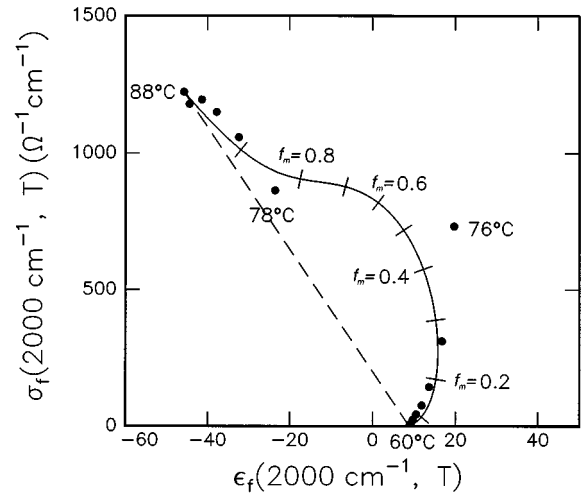


FIG. 9. Comparisons of the dielectric constant and conductivity of the VO<sub>2</sub> film at 2000 cm<sup>-1</sup>. Solid circles represent the experimental data and the solid line shows the prediction of the two-dimensional EMA. The dashed line shows the prediction of the Maxwell Garnet theory (Ref. 40), which is a mean-field theory without the percolation transition.

based on a homogeneous medium will fail to explain behaviors of many physical properties correctly.

## V. SUMMARY

Temperature-dependent mid-IR transmittance and reflectance spectra of a VO<sub>2</sub> film were measured near MI transition. Using the ITMM, the conductivity and dielectric constant of the film were obtained between 1600 and 4000 cm<sup>-1</sup>. Above 78 °C,  $\epsilon_f(\omega)$  and  $\sigma_f(\omega)$  showed a typical metallic behavior. The optical constants in the metallic region can be explained in terms of the extended Drude model. The dc mean free path is estimated to be much larger than the previously reported value. In the insulating region,  $\epsilon_f(\omega)$  increased as  $T$  approached the MI transition temperature, contrary to an expectation based on the fact that the number of carriers increases homogeneously over the film. To explain this anomalous behavior near the transition, the film in the transition region was approximated as a composite consisted of metallic and insulating VO<sub>2</sub> domains and the effective-medium approximation was applied. Then the dielectric anomaly was attributed to increase in capacitive coupling between the metallic grains near the percolation threshold.

## ACKNOWLEDGMENTS

We appreciate the ICNSRF for allowing us to use their facilities. This work was financially supported by the Ministry of Education through the Basic Science Research Institute Program No. BSRI-95-2416 and by the Korea Science and Engineering Foundation through the RCDAMP at Pusan National University.

- \*Electronic address: twnoh@phya.snu.ac.kr  
 † Present address: LG Electronic Research Center, Seoul 137-140, Korea.
- <sup>1</sup>F. J. Morin, Phys. Rev. Lett. **3**, 34 (1959).
  - <sup>2</sup>A. S. Barker, Jr., H. W. Verleur, and H. J. Guggenheim, Phys. Rev. Lett. **17**, 1286 (1966).
  - <sup>3</sup>H. W. Verleur, A. S. Barker, Jr., and C. N. Berglund, Phys. Rev. **172**, 788 (1968).
  - <sup>4</sup>F. Gervais and W. Kress, Phys. Rev. B **31**, 4809 (1985).
  - <sup>5</sup>D. B. McWhan, M. Marezio, J. P. Remeika, and P. D. Dernier, Phys. Rev. B **10**, 490 (1974).
  - <sup>6</sup>M. Abbate, F. M. F. de Groot, J. C. Fuggle, Y. J. Ma, C. T. Chen, F. Sette, A. Fujimori, Y. Ueda, and K. Kosuge, Phys. Rev. B **43**, 7263 (1991).
  - <sup>7</sup>C. N. Berglund and H. J. Guggenheim, Phys. Rev. **185**, 1022 (1969).
  - <sup>8</sup>A. Zylbersztein and N. F. Mott, Phys. Rev. B **11**, 4383 (1975).
  - <sup>9</sup>I. A. Abroyan, V. Ya. Velichko, and F. A. Chudnovskii, Fiz. Tverd. Tela (Leningrad) **27**, 1667 (1985) [Sov. Phys. Solid State **27**, 1002 (1985)].
  - <sup>10</sup>D. Alder and H. Brooks, Phys. Rev. **155**, 826 (1967).
  - <sup>11</sup>J. Goodenough, Solid State Chem. **3**, 490 (1971).
  - <sup>12</sup>D. Paquet, Phys. Rev. B **22**, 5284 (1980).
  - <sup>13</sup>R. M. Wentzcovitch, W. W. Schulz, and P. B. Allen, Phys. Rev. Lett. **72**, 3389 (1994); T. M. Rice, H. Launois, and J. P. Pouget, *ibid.* **73**, 3042 (1994); R. M. Wentzcovitch, W. W. Schulz, and P. B. Allen, *ibid.* **73**, 3043 (1994).
  - <sup>14</sup>D. H. Kim and H. S. Kwok, Appl. Phys. Lett. **65**, 3188 (1994).
  - <sup>15</sup>To check the reproducibility of our measurements, the transmittance spectra were measured repeatedly during several thermal cycles. It was found that there were few differences in the measured transmittances and that such differences could be explained in terms of a temperature difference of about 0.5 °C.
  - <sup>16</sup>E. E. Chain, Appl. Opt. **30**, 2782 (1991).
  - <sup>17</sup>F. C. Case, Appl. Opt. **30**, 4119 (1991).
  - <sup>18</sup>C. Kittel, *Introduction to Solid State Physics*, 6th ed. (Wiley, New York, 1986).
  - <sup>19</sup>F. Wooten, *Optical Properties of Solids* (Academic, New York, 1972).
  - <sup>20</sup>R. M. A. Azzam and N. M. Bashara, *Ellipsometry and Polarized Light* (North-Holland, Amsterdam, 1977).
  - <sup>21</sup>C. J. Gabriel and A. Nedoluha, Opt. Acta **18**, 415 (1971).
  - <sup>22</sup>T. W. Noh, P. H. Song, Sung-Ik Lee, D. C. Harris, J. R. Gaines, and J. C. Garland, Phys. Rev. B **46**, 4212 (1992).
  - <sup>23</sup>H. S. Choi, J. S. Ahn, W. Jo, and T. W. Noh, J. Korean Phys. Soc. **28**, 636 (1995).
  - <sup>24</sup>I. H. Malitson, F. V. Murphy, and W. S. Rodeny, J. Opt. Soc. Am. **48**, 72 (1958).
  - <sup>25</sup>A. S. Barker, Phys. Rev. **132**, 1474 (1963).
  - <sup>26</sup>M. E. Thomas, R. I. Joseph, and W. J. Tropf, Appl. Opt. **27**, 239 (1988).
  - <sup>27</sup>*Handbook of Optical Constants of Solids II*, edited by E. D. Palik (Academic, San Diego, 1991).
  - <sup>28</sup>S. Onari, T. Arai, and K. Kudo, Phys. Rev. B **16**, 1717 (1977).
  - <sup>29</sup>Similar curves for  $\sigma_f(\omega, T)$  and  $\epsilon_f(\omega, T)$  were also obtained for the  $\mathcal{R}$  and  $\mathcal{T}$  data during the cooling process, but with a temperature difference of 8 °C. Due to the similarity, the data for the cooling process are omitted in this paper.
  - <sup>30</sup>To explain the optical properties of some metal oxides, including the high- $T_c$  superconductors, many workers have used a two-component model, which considers the free-carrier and mid-IR absorption contributions for  $\sigma(\omega)$ . Refer to T. Timusk and D. B. Tanner, in *The Physical Properties of High Temperature Superconductors*, edited by D. M. Ginsberg (World Scientific, Singapore, 1989). We tried to use this model, but failed to get a good description for our measured optical constants.
  - <sup>31</sup>B. C. Webb, A. J. Sievers, and T. Mihalisin, Phys. Rev. Lett. **57**, 1951 (1986).
  - <sup>32</sup>Y. Fujishima, Y. Tokura, T. Arima, and S. Uchida, Phys. Rev. B **46**, 11 167 (1992).
  - <sup>33</sup>N. W. Ashcroft and N. D. Mermin, *Solid State Physics* (Saunders, Philadelphia, 1976), Appendix A.
  - <sup>34</sup>P. B. Allen, R. M. Wentzcovitch, W. W. Schulz, and P. C. Canfield, Phys. Rev. B **48**, 4359 (1993).
  - <sup>35</sup>K. F. Herzfeld, Phys. Rev. **29**, 701 (1927).
  - <sup>36</sup>T. V. Ramakrishnan, in *The Metallic and Nonmetallic States of Matter*, edited by P. P. Edwards and C. N. R. Rao (Taylor & Francis, London, 1985).
  - <sup>37</sup>T. W. Noh, Y. Song, S.-I. Lee, J. R. Gaines, H. D. Park, and E. R. Kreidler, Phys. Rev. B **33**, 3793 (1986).
  - <sup>38</sup>D. Bruggemann, Ann. Phys. (Leipzig) **24**, 636 (1935).
  - <sup>39</sup>D. Stroud, Phys. Rev. B **12**, 3368 (1975).
  - <sup>40</sup>Another effective-medium theory, called the Maxwell-Garnett theory (MGT), has also been widely used. Refer to J. C. Maxwell Garnett, Philos. Trans. R. Soc. London **203**, 385 (1904). However, since the MGT does not predict the percolation transition, it fails to describe the evolution of the domain growth shown in Fig. 7.
  - <sup>41</sup>T. W. Noh, P. H. Song, and A. J. Sievers, Phys. Rev. B **44**, 5459 (1991).
  - <sup>42</sup>Note that the reflectance and transmittance spectra, displayed in Figs. 1(b) and 2, show rather continuous changes, contrary to the behaviors of  $\epsilon_f(\omega, T)$  and  $\sigma_f(\omega, T)$ .
  - <sup>43</sup>D. M. Grannan, J. C. Garland, and D. B. Tanner, Phys. Rev. Lett. **46**, 375 (1981).
  - <sup>44</sup>Near the percolation transition, a typical size of metallic clusters relative to the wavelength of light might also play an important role, as demonstrated by a scaling theory based on the conductivity fluctuation. For reference, see Yagil *et al.*, Phys. Rev. B **43**, 11 342 (1991) and Ref. 22.